communications biology

Article

https://doi.org/10.1038/s42003-025-07545-7

Positively charged cytoplasmic residues in corin prevent signal peptidase cleavage and endoplasmic reticulum retention

Check for updates

Hui Li[1,2,4], Shijin Sun[1,2,4], Wenjun Guo[1,3,4], Lina Wang[1], Zihao Zhang[1,3], Yue Zhang[1,2], Ce Zhang[1,2], Meng Liu[1], Shengnan Zhang[1,3], Yayan Niu[1,3], Ningzheng Dong[1,3] ✉ & Qingyu Wu[1] ✉

Positively charged residues are commonly located near the cytoplasm-membrane interface, which is known as the positive-inside rule in membrane topology. The mechanism underlying the function of these charged residues remains poorly understood. Herein, we studied the function of cytoplasmic residues in corin, a type II transmembrane serine protease in cardiovascular biology. We found that the positively charged residue at the cytoplasm-membrane interface of corin was not a primary determinant in membrane topology but probably served as a charge-repulsion mechanism in the endoplasmic reticulum (ER) to prevent interactions with proteins in the ER, including the signal peptidase. Substitution of the positively charged residue with a neutral or acidic residue resulted in corin secretion likely due to signal peptidase cleavage. In signal peptidase-deficient cells, the mutant corin proteins were not secreted but retained in the ER. Similar results were found in the low-density lipoprotein receptor and matriptase-2 that have positively charged residues at and near the cytoplasm-membrane interface. These results provide important insights into the role of the positively charged cytoplasmic residues in mammalian single-pass transmembrane proteins.

Membrane proteins are of major biological importance. In humans, ~6000 of the >21,000 annotated genes are predicted to encode membrane proteins[1,2]. Among them, ~50% are expected to be single-pass transmembrane proteins, including transporters, receptors, enzymes, ligand-binding proteins, and adhesion molecules[1,3–5]. These proteins are oriented on the cell membrane with a C- (type I) or N-terminal (type II) cytoplasmic segment.

Charged residues flanking the membrane-spanning segment are recognized as key determinants in membrane topology[6–8]. As indicated by the positive-inside rule, positively charged residues are enriched at or near the cytoplasm-membrane interface[9–11]. The presence of more positively charged residues immediately preceding the transmembrane segment predicts the N-terminus-inside orientation, whereas the presence of more positively charged residues immediately following the transmembrane segment predicts the C-terminus-inside orientation. This rule applies to most transmembrane proteins in virtually all organisms, ranging from bacteria to humans[12,13]. Currently, the charge residue distribution bias is used as one of the key parameters in computer algorithms for membrane topology prediction[14,15]. It remains unclear, however, how the positively charged cytoplasmic residues contribute to the membrane topology of the transmembrane proteins.

Corin is a type II transmembrane serine protease expressed in diverse tissues, including the heart, kidney, skin, and uterus[16–20], where it activates atrial natriuretic peptide (ANP) to control body fluid and cardiovascular homeostasis[21–23]. Corin-mediated ANP activation also plays an important role in regulating adipocyte differentiation, energy metabolism, thermogenesis, and bone development[24–28]. In humans, altered corin expression and/or function have been implicated in major cardiovascular diseases, including hypertension, preeclampsia, cardiac hypertrophy and fibrosis, heart failure, atrial fibrillation, and stroke[29–35].

Like many single-pass transmembrane proteins, corin has a positively charged residue at the cytoplasm-membrane interface[16]. Previously, we found that cytoplasmic sequences are important for corin expression on the cell surface[36,37]. A *CORIN* variant in hypertensive patients, deleting 30 N-terminal residues in the cytoplasmic tail, which might create a potential myristoylation site, impaired corin intracellular trafficking and ANP activation[36,38]. It remains unknown whether the positively charged cytoplasmic residues regulate corin membrane

[1]Cyrus Tang Hematology Center, Collaborative Innovation Center of Hematology, State Key Laboratory of Radiation Medicine and Prevention, Suzhou Medical College, Soochow University, Suzhou, 215123, China. [2]Affiliated Suzhou Hospital of Nanjing Medical University, Suzhou Municipal Hospital, Suzhou, 215002, China. [3]NHC Key Laboratory of Thrombosis and Hemostasis, Jiangsu Institute of Hematology, The First Affiliated Hospital of Soochow University, Suzhou, China. [4]These authors contributed equally: Hui Li, Shijin Sun, Wenjun Guo. ✉e-mail: ningzhengdong@suda.edu.cn; wuqy@suda.edu.cn

topology. In this study, we examined the functional significance of the positively charged cytoplasmic residues in corin. Our results may provide new insights into the role of the positively charged cytoplasmic residues in mammalian single-pass transmembrane proteins.

Results

Minimal cytoplasmic residues required for corin expression on the cell surface

Corin is a multiple-domain protease synthesized as a one-chain zymogen (Fig. 1a). Proprotein convertase subtilisin/kexin 6 (PCSK6) cleaves corin, converting it to a two-chain active enzyme tethered on the cell surface by a disulfide bond[39] (Fig. 1a). When murine wild-type corin (mWT) was expressed in human embryonic kidney 293 (HEK293) cells and analyzed by western blotting under non-reducing conditions with an anti-C-terminal V5 tag antibody, the protein was detected as an ~180-kDa band, representing the zymogen and activated corin (Fig. 1b, left panel). Under reducing conditions, which break disulfide bonds, corin was detected as an ~180-kDa band and an ~40-kDa band, representing the one-chain zymogen and the cleaved protease domain fragment (Cor-p), respectively (Fig. 1b, right panel). PCSK6 activates corin on the cell surface, but not intracellularly[39]. When cell surface proteins were digested by trypsin before the cells were lysed, the Cor-p band was not detected in western blotting (Fig. 1c). Thus, the Cor-p band can serve as an indicator for corin expression and activation on the cell surface.

The cytoplasmic tail of murine corin consists of 112 residues, including two positively charged residues, Lys104 and Arg112, in the juxtamembrane region[37] (Fig. 1a). We examined the minimal cytoplasmic length required for corin expression on the cell surface in a set of truncation mutants (Fig. 1a). When the cytoplasmic tail was shortened to fourteen (Δ1), seven (Δ2), and two (Δ3) residues, respectively, the Cor-p band was detected by western blotting in transfected HEK293 cells expressing the mutants (Fig. 1d, e), indicating that these mutants were expressed on the cell surface. In contrast, the Cor-p band was not detected in Δ4 mutant with only the initiation Met in the cytoplasmic tail (Fig. 1a, e). These results were confirmed by immunostaining (Fig. 1f) and flow cytometry (Fig. 1g and Supplementary Fig. 1a, b), showing the expression of mWT and the Δ3 mutant, but not the Δ4 mutant, on the cell surface.

Importance of the positively charged residue at the cytoplasm-membrane interface

To understand whether the difference in cell surface expression between the Δ3 and Δ4 mutants was due to the cytoplasmic length or the presence of a positively charged residue at the cytoplasm-membrane interface, we tested another set of corin mutants, in which the cytoplasmic Arg in the Δ3 mutant was replaced by Ala (neutral) (Δ3 R/A), Asp (negatively charged) (Δ3 R/D), or Lys (positively charged) (Δ3 R/K), respectively (Fig. 2a). In western blotting of cell lysates under reducing conditions, the Cor-p band was detected in mWT and the mutants Δ3 and Δ3 R/K, but not the mutants Δ4, Δ3 R/A, and Δ3 R/D (Fig. 2b). Similar results were found in western blotting

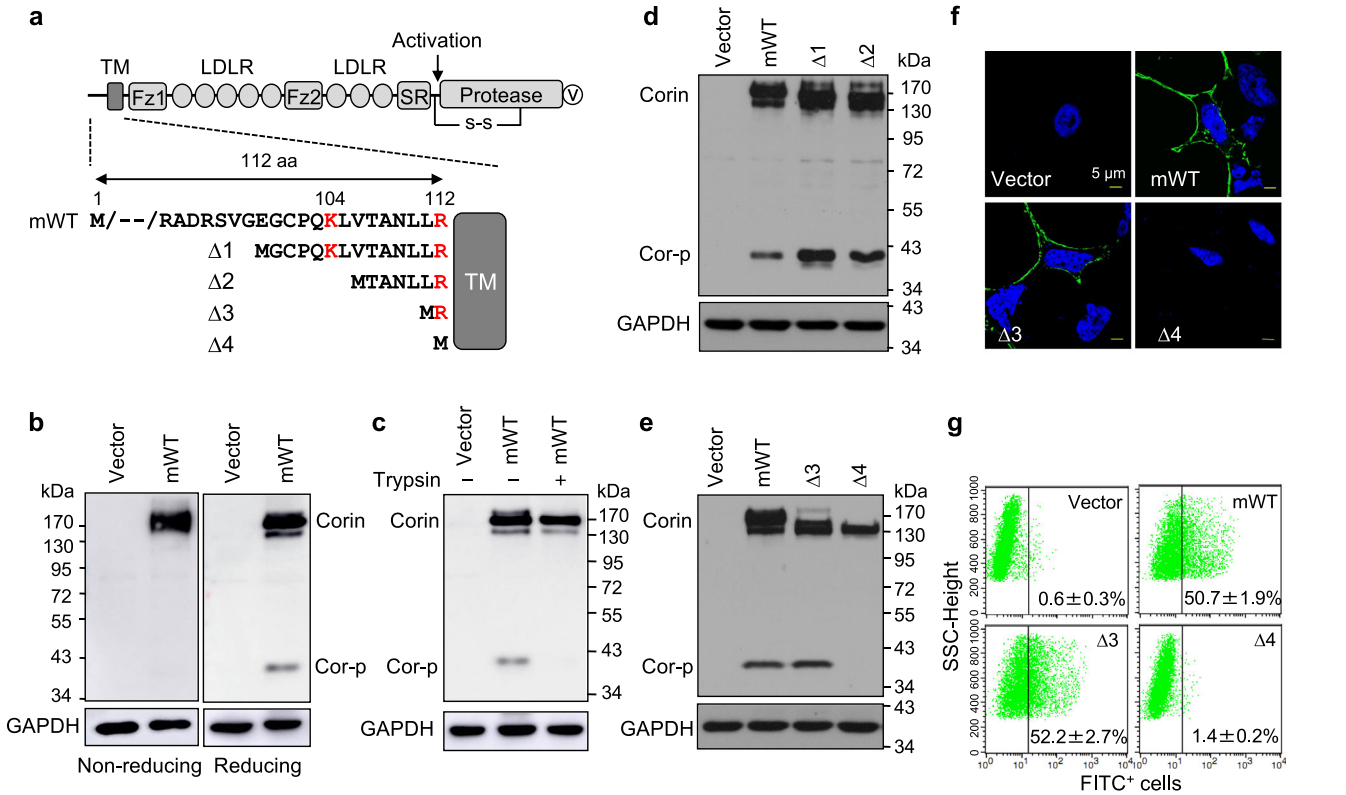

Fig. 1 | Activation cleavage and cell surface expression of mouse corin mutants with shortened cytoplasmic tails. a Corin protein domains and plasmids expressing mouse WT corin (mWT) with a 112-amino-acid cytoplasmic tail and mutants with shortened cytoplasmic tails (Δ1-Δ4). TM, transmembrane; Fz, frizzled; LDLR, LDL receptor, SR, scavenger receptor. The activation cleavage site (arrow), a disulfide bond (s-s) between the stem region and the protease domain, and a C-terminal V5 (v) tag are indicated. **b** Western blotting of mWT in HEK293 cell lysates under non-reducing (left) and reducing (right) conditions. The full-length corin (Corin) and the activation cleaved corin protease domain (Cor-p) are indicated. GAPDH was a control. Data are representative of four experiments. **c** Western blotting of mWT in transfected cells without (−) or with (+) trypsin digestion. Western blotting was under reducing conditions. Data are representative of three experiments. **d, e** Western blotting of mWT and corin mutants from transfected cells under reducing conditions. Data are representative of five experiments. **f** Immunostaining of corin proteins on the surface of non-membrane permeabilized cells. Scale bars, 5 μm. Data are representative of five experiments. **g** Flow cytometric analysis of corin protein on the cell surface. Percentages of corin-positive cells are indicated. $n = 5$ per group.

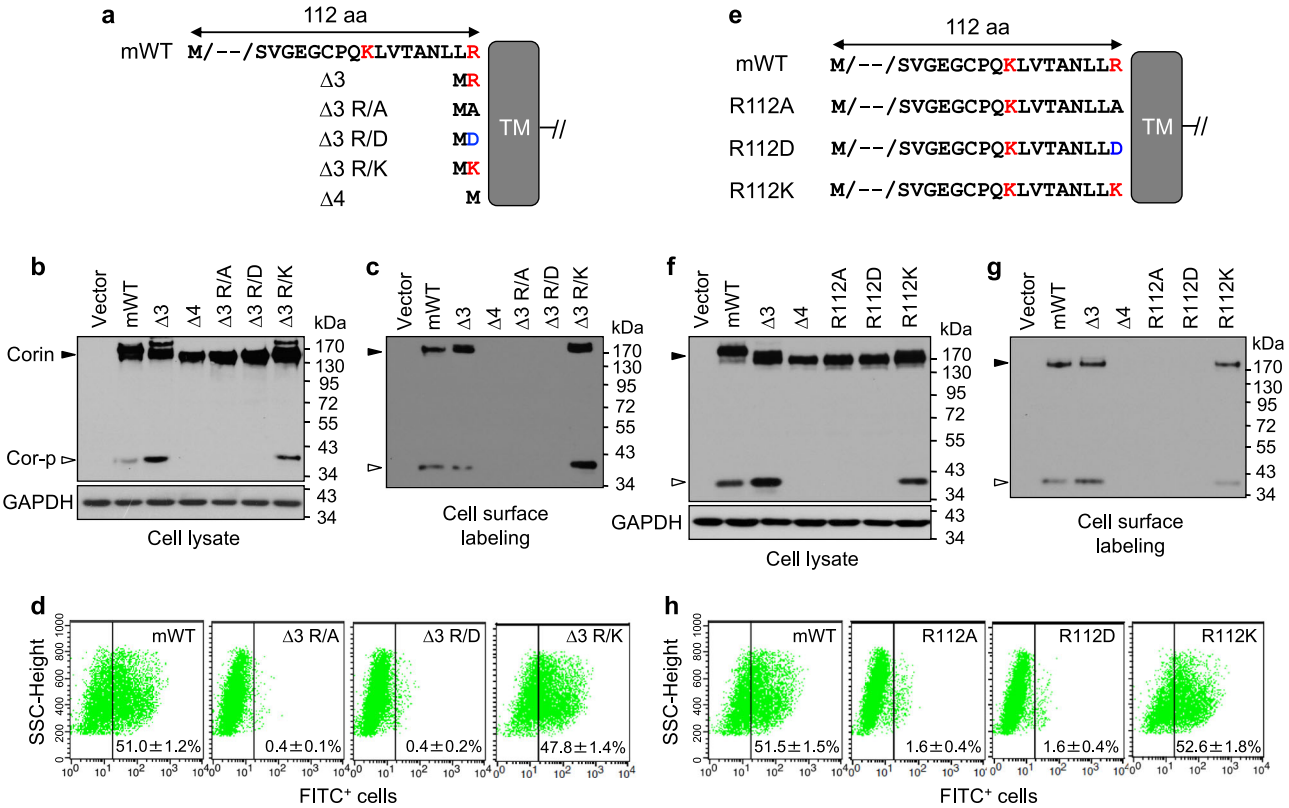

Fig. 2 | Activation cleavage and cell surface expression of mouse corin mutants with substituted residues at the cytoplasm-membrane interface. a Mouse corin mutants with altered cytoplasmic sequences. Corin extracellular domains are not shown. TM, transmembrane. **b** Western blotting of corin proteins from transfected cells under reducing conditions. Data are representative of five experiments. **c** Western blotting of biotin-labeled cell surface corin proteins under reducing conditions. Data are representative of three experiments. **d** Flow cytometric analysis of corin on the cell surface. Percentages of corin-positive cells are indicated. $n = 6$ per group. **e** Mouse corin mutants with a full-length cytoplasmic tail. Western blotting of corin proteins in lysates (**f**) and biotin-labeled cell surface proteins (**g**) from transfected cells. Western blotting was done under reducing conditions. Data are representative of three experiments. **h** Flow cytometric analysis of corin proteins on the cell surface. Percentages of corin-positive cells are indicated. $n = 6$ per group.

of biotin-labeled cell surface proteins (Fig. 2c). In flow cytometry, which was more quantitative, mWT and the Δ3 R/K mutant, but not the Δ3 R/A and Δ3 R/D mutants, were detected on the cell surface (Fig. 2d and Supplementary Fig. 1c). These results indicated that a positively charged residue at the cytoplasm-membrane interface was required for corin expression on the cell surface.

We verified the results in full-length murine corin mutants, in which Arg112 was replaced by Ala (R112A), Asp (R112D), or Lys (R112K), respectively (Fig. 2e). In western blotting of lysates from transfected cells, the Cor-p band was detected in mWT and the mutants Δ3 and R112K, but not the mutants Δ4, R112A, and R112D (Fig. 2f). Consistently, mWT and the mutants Δ3 and R112K, but not the mutants Δ4, R112A, and R112D, were detected by western blotting in biotin-labeled cell surface proteins (Fig. 2g). In flow cytometry, levels of mWT and the mutant R112K on the cell surface were similar, whereas levels of the mutants R112A and R112D were barely detectable (Fig. 2h and Supplementary Fig. 1d). These data indicated that, regardless the length of the cytoplasmic tail, a positively charged residue at the cytoplasm-membrane interface was necessary for corin cell surface expression.

Importance of positively charged cytoplasmic residues in human corin

The cytoplasmic tail of human corin differs from that of murine corin in length and sequence due to the use of an alternative exon[37]. To verify our findings, we tested the importance of cytoplasmic Lys37 and Arg45 in human corin (hWT) (Fig. 3a). We made a set of mutants, in which Lys37 and Arg45 were mutated to Ala, individually or together (Fig. 3a), and analyzed the mutants in transfected cells by western blotting. The Cor-p band was detected in hWT and the mutants R45A, K37A, and K37A/R45A (Fig. 3b). However, levels of the band in the mutants R45A and K37A/R45A were lower than those in hWT and the mutant K37A, as assessed by the ratio of the Cor-p band vs. the zymogen band (Corin) (Fig. 3b, c). The results indicated that the cell surface expression and activation of human corin were reduced in the mutants R45A and K37A/R45A, suggesting that a positively charged residue at the cytoplasm-membrane interface was more important than one at a more distant location.

Consistently, substitution of Arg45 with Asp (R45D) or Glu (R45E), but not Lys (R45K) or His (R45H), decreased human corin expression and zymogen activation on the cell surface, as indicated by reduced levels of the Cor-p band in western blotting of lysates from transfected cells (Fig. 3a, d). Similar results were observed in flow cytometric analysis of cell surface corin (Fig. 3e and Supplementary Fig. 1d). Reduced cell surface expression of the mutant R45A was also confirmed in these experiments (Fig. 3d, e and Supplementary Fig. 1e).

Effects of cytoplasmic residues on corin membrane topology

Positively charged cytoplasmic residues are known determinants in membrane topology. Possibly, the substitution of the Arg at the cytoplasm-membrane interface with a neutral or negatively charged residue may reverse the membrane orientation of corin (Fig. 4a). As corin was activated extracellularly and the antibody used in western blotting was against a C-terminal tag, the reversed membrane topology might explain the observed results. To exclude this possibility, we examined N-glycans on corin proteins, as N-glycosylation occurs in the endoplasmic reticulum (ER)

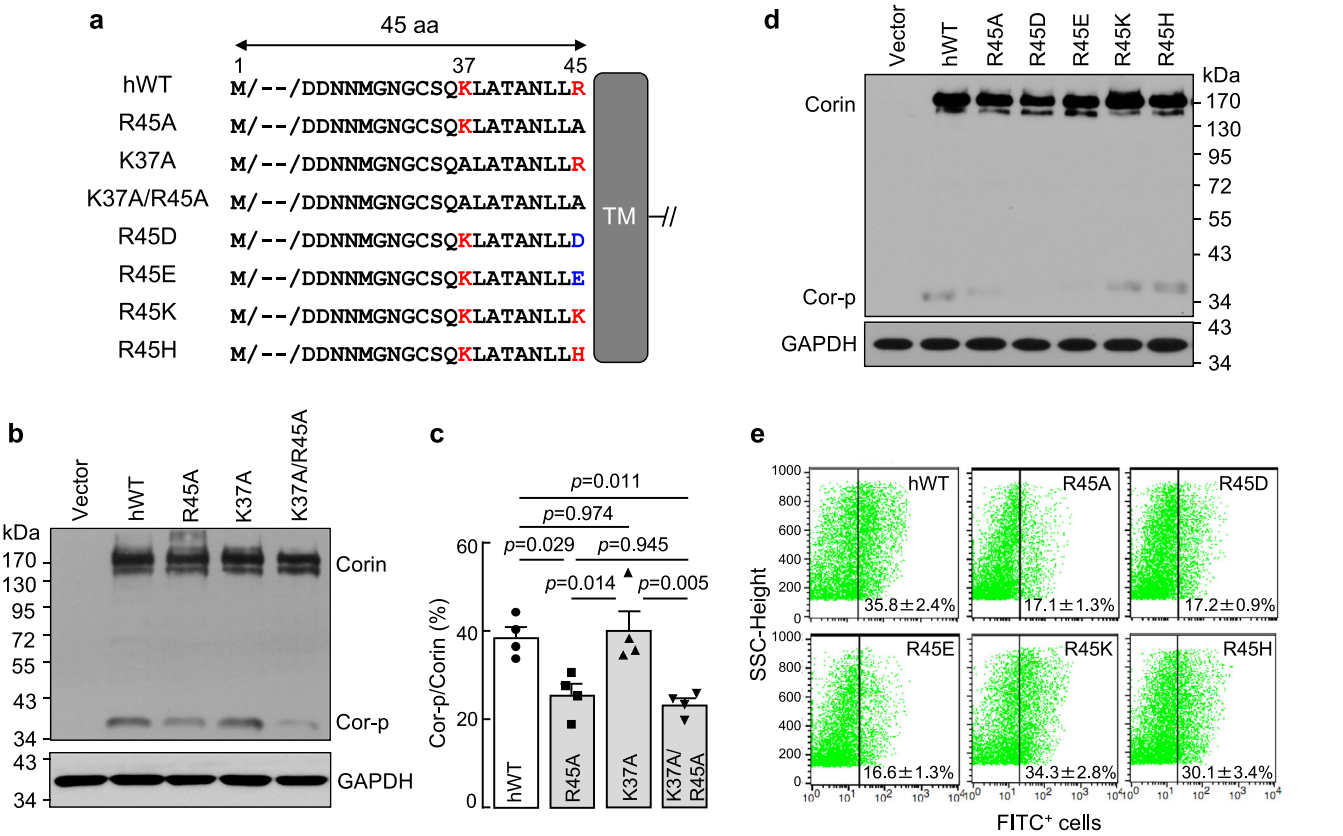

Fig. 3 | Activation cleavage and cell surface expression of full-length human corin mutants with substituted residues at the cytoplasm-membrane interface. a Full-length human corin mutants with altered cytoplasmic residues. Corin extracellular domains are not shown. TM, transmembrane. **b** Western blotting of human corin proteins from transfected cells under reducing conditions. Data are representative of four experiments. **c** Quantitative data of corin activation cleavage, as measured by the ratio of Cor-p *vs.* Corin bands from densitometric analysis of western blots. $n = 4$. *P* values were analyzed by one-way ANOVA. **d** Western blotting of human corin mutants from transfected cells under reducing conditions. Data are representative of three experiments. **e** Flow cytometric analysis of corin proteins on the cell surface. Percentages of corin-positive cells are indicated. $n = 4$ per group.

lumen. We treated corin proteins in cell lysates with PNGase F to eliminate N-glycans and analyzed the proteins by western blotting. We found that mWT and the mutants Δ3 R/A, Δ3 R/D, Δ3 R/K, R112A, R112D, and R112K all migrated faster after PNGase F treatment (Fig. 4b, c), indicating that these proteins were N-glycosylated and hence in the type II membrane orientation.

Secretion of corin mutants into the conditioned media

We next examined corin proteins in the conditioned media from the transfected cells. As reported previously[40], corin is shed from the cell surface by a disintegrin and metalloproteinase 10 (ADAM10)-mediated cleavage in the external juxtamembrane region, generating an ~180-kDa fragment, and by self-cleavages in frizzed 1 (Fz1) and low-density lipoprotein receptor 5 (LDLR5) domains, generating an ~160-kDa fragment and an ~110-kDa fragment, respectively (Fig. 4d). As a control, we included a soluble corin (sCorin), in which the cytoplasmic tail and the transmembrane domain were replaced with a signal peptide[41] (Fig. 4d).

By western blotting, we detected the ~180-, ~160-, and ~110-kDa fragments in the conditioned medium from the cells expressing mWT, consistent with previous findings[40] (Fig. 4e, top panel). Similar fragments were observed in the conditioned medium from the cells expressing the mutant Δ3 R/K. In contrast, only an ~160-kDa fragment was found in the conditioned media from the cells expressing the mutants Δ3 R/A and Δ3 R/D. As expected, an ~160-kDa fragment was detected in the conditioned medium from sCorin-expressing cells (Fig. 4e, top panel). In cell lysates, the Cor-p band was detected in mWT and the mutant Δ3 R/K, but not the Δ3 R/A and Δ3 R/D mutants and sCorin (Fig. 4e, middle panel). These results indicated that, like sCorin, the mutants Δ3 R/A and Δ3 R/D were secreted into the medium, which could explain the lack of cell surface expression and the Cor-p band (i.e., activation) in cell lysates.

Cleavage of corin mutants by the signal peptidase

The signal peptidase complex (SPC) in the ER is critical for protein secretion[42–44]. In humans, there are two SPC paralogs, consisting of an alternative catalytic subunit SPC18 or SPC21 and three common subunits SPC12, SPC22/23, and SPC25[45] (Supplementary Fig. 2a). Both SPC18 and SPC21 are type II transmembrane proteins with positively charged residues at the cytoplasm-membrane interface (Supplementary Fig. 2a)[45]. Possibly, the positively charged residue at the cytoplasm-membrane interface of corin prevents the SPC-mediated cleavage in a charge-repulsion mechanism (Fig. 5a). When the cytoplasmic Arg is replaced by another positively charged residue, this mechanism is preserved and the corresponding corin mutants remain membrane-bound. When the Arg residue is deleted or replaced with an Ala or negatively charged residue, this repulsion mechanism is abolished, resulting in signal peptidase cleavage and corin secretion from the cell (Fig. 5a).

To test this hypothesis, we generated mutant HEK293 cell lines, in which the *SEC11A* gene, encoding SPC18, or the *SEC11C* gene, encoding SPC21, was disrupted by CRISPR-Cas9 (Supplementary Figs. 2b-d and 3a-c). When mWT and the mutants Δ3 and Δ4 were expressed in these cells and analyzed by western blotting, we detected fragments from mWT and the mutants Δ3 and Δ4 in the conditioned media from parental HEK293

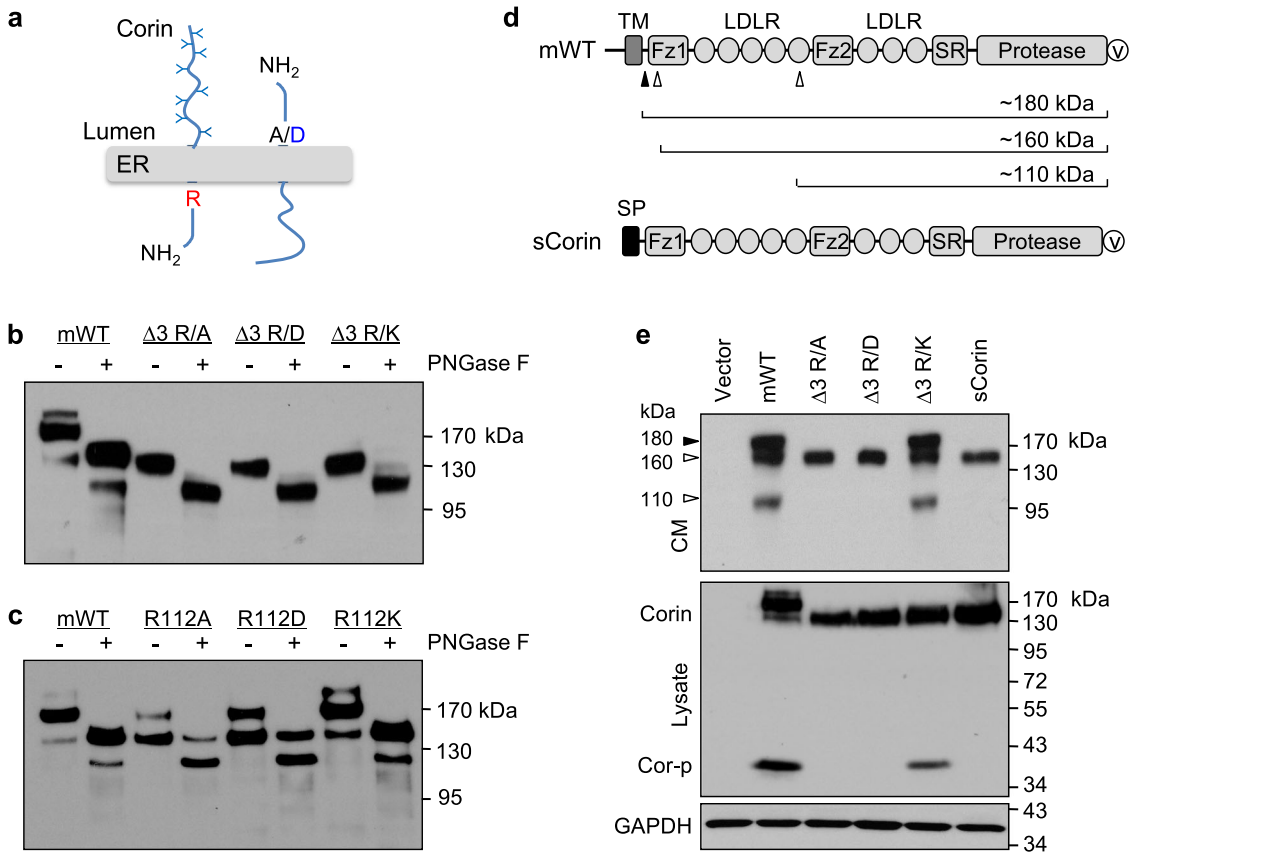

Fig. 4 | N-glycosidase digestion and detection of corin proteins in the conditioned media. a Alternative corin membrane orientations in the ER. WT corin with the cytoplasmic Arg (R) (left) and the mutants, in which the Arg was replaced by Ala (A) or Asp (D) (right). NH_2, N-terminus. Y shaped symbols indicate N-glycans. **b, c** Western blotting of corin proteins from transfected cells without (−) or with (+) PNGase F treatment. Western blotting was done under reducing conditions. Data are representative of three experiments. **d** Illustration of cleaved corin ectodomain fragments. The ADAM10 cleavage site (filled arrowhead) and corin autocleavage sites (open arrowheads) and corresponding cleaved fragments are indicated. A soluble corin (sCorin), in which the cytoplasmic tail and the transmembrane domain were replaced with a signal peptide (SP), was a control. **e** Western blotting of corin proteins in the conditioned media (CM) (top panel) and cell lysates (middle panel) from transfected cells. In the top panel, ADAM10-cleaved and corin self-cleaved fragments in mWT are indicated by filled and open arrowheads, respectively. GAPDH in cell lysates was a control (bottom panel). Data are representative of three experiments.

cells (Fig. 5b, top panel, lanes 2-4 and Supplementary Fig. 4a). In contrast, fragments from mWT and the Δ3 mutant, but not the Δ4 mutant, were detected in the conditioned media from SPC18 knockout (SPC18 KO) cells (Fig. 5b, top panel, lanes 6-8 and Supplementary Fig. 4a). In cell lysates, comparable levels of mWT and the mutants Δ3 and Δ4 were observed in both HEK293 and SPC18 KO cells, but the Cor-p band was detected only in mWT and the Δ3 mutant (Fig. 5b, middle panel). In parallel experiments, fragments from mWT and the mutants Δ3 R/A, Δ3 R/D, and Δ3 R/K were detected in the conditioned media from HEK293 cells (Fig. 5c, top panel, lanes 2-5 and Supplementary Fig. 4b), but only fragments from mWT and the Δ3 R/K mutant were detected in the conditioned media from SPC18 KO cells (Fig. 5c, top panel, lanes 7-10 and Supplementary Fig. 4b). In cell lysates, comparable levels of all corin proteins were observed in HEK293 and SPC18 KO cells, but the Cor-p band was not detected in the mutants Δ3 R/A and Δ3 R/D (Fig. 5c, middle panel). In similar experiments, fragments from mWT and the mutants Δ3 and Δ4 were detected in the conditioned media from both HEK293 and SPC21 KO cells (Supplementary Fig. 3d). These results indicated that the mutants Δ4, Δ3 R/A, and Δ3 R/D, but not the Δ3 R/K mutant, were probably cleaved by the SPC paralog with SPC18, but not SPC21, catalytic subunit (Fig. 5a).

To verify our findings and to distinguish the secreted corin fragment from that of the self-cleaved fragment at ~160 kDa[40] (Supplementary Fig. 5a), we mutated the active Ser in mWT (mWT S1052A) and made corresponding mutants Δ4 S1052A, Δ3 R/A S1052A, and Δ3 R/D S1052A (Supplementary Fig. 5a,b). In western blotting of corin proteins in the conditioned media from the transfected HEK293 cells, we detected the ~180-kDa (from ADAM10 cleavage), ~160 and ~110-kDa (from corin autocleavage) fragments from mWT[40], but only the ~180-kDa fragment from mWT S1052A, as expected (Supplementary Fig. 5c, top panel). There was only the ~160-kDa fragment detected from the mutants Δ4, Δ3 R/A, Δ3 R/D, Δ4 S1052A, Δ3 R/A S1052A, and Δ3 R/D S1052A (Supplementary Fig. 5c, top panel). In the cell lysates, the Cor-p band was detected only in mWT and mWT S1052A (Supplementary Fig. 5c, middle panel). These results were consistent, indicating that the ~160-kDa fragment in the conditioned media from Δ4, Δ3 R/A, and Δ3 R/D mutants was from secretion but not corin autocleavage.

Retention of corin mutants in the ER of SPC18 KO cells

To understand the fate of the mutants Δ4, Δ3 R/A, and Δ3 R/D in SPC18 KO cells, we did co-immunostaining of KDEL (ER marker) and corin proteins in HEK293 and SPC18 KO cells. There was little overlapping staining between KDEL and mWT or the mutant corin proteins in HEK293 cells (Fig. 5d, top row, and Supplementary Fig. 6a, b). However, there was strong co-staining between KDEL and the Δ4, Δ3 R/A, and Δ3 R/D mutants, but not mWT and the mutant Δ3 R/K, in SPC18 KO cells (Fig. 5d, second row, and Supplementary Fig. 6a, b). In contrast, there was no apparent co-staining between GM130 (Golgi marker) and mWT or the mutant proteins in HEK293 or SPC18 KO cells (Fig. 5d, third and bottom rows, and Supplementary Fig. 6c, d). In flow cytometry, we detected mWT and the mutant Δ3 R/K, but not the mutants Δ3 R/A and Δ3 R/D, on the

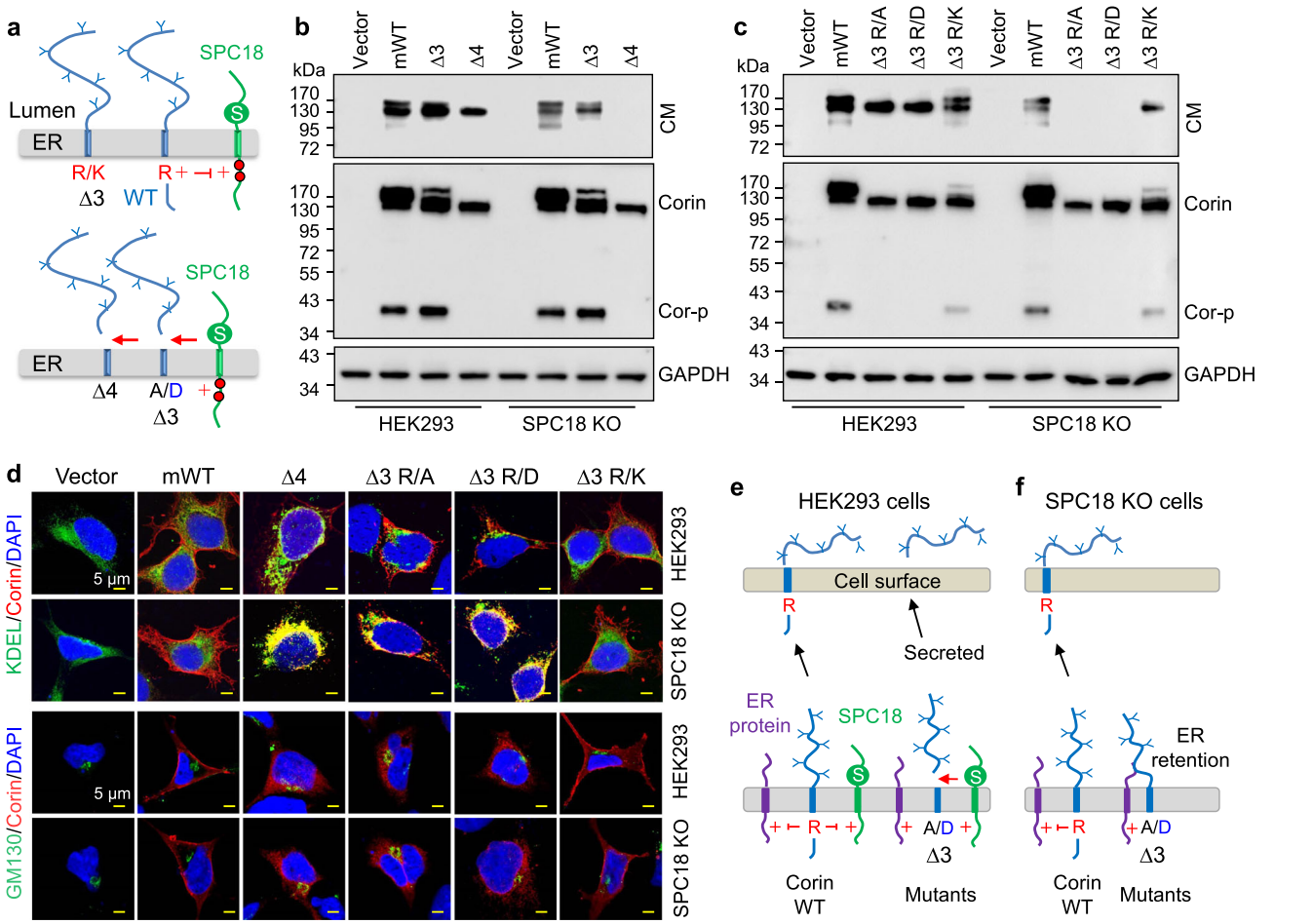

Fig. 5 | Analysis of corin proteins in HEK293 and SPC18 KO cells. a A proposed model. WT corin and the mutants Δ3 and Δ3 R/K had a positively charged Arg (R) or Lys (K) at the cytoplasm-membrane interface, preventing cleavage by SPC18 with the active Ser (S) and positively charged cytoplasmic residues (red dots). The mutants Δ4, Δ3 R/A, and Δ3 R/D lacking the positively charged cytoplasmic residue were cleaved by SPC18 (arrows). Western blotting of corin fragments in the conditioned media (CM) (top panels) and lysates (bottom panels) from HEK293 and SPC18 KO cells expressing mWT and the mutants Δ3 and Δ4 (**b**), or Δ3 R/A, Δ3 R/D, and Δ3 R/K (**c**). Data are representative of at least four experiments. **d** Co-straining of KDEL or GM130 and corin in HEK293 and SPC18 KO cells expressing mWT and the corin mutants. Nuclei were stained with DAPI. Scale bars: 5 μm. Data are representative of at least six experiments. **e, f** A proposed model. In HEK293 cells, the cytoplasmic Arg protects WT corin from interacting with SPC18 and ER proteins with positively charged cytoplasmic residues, allowing corin expression on the cell surface. When the cytoplasmic Arg is replaced by Ala (A) or Asp (D), the mutants were cleaved by SPC18 and secreted from HEK293 cells or trapped by ER proteins in SPC18 KO cells.

surface of HEK293 and SPC18 KO cells (Supplementary Fig. 6e). These results indicated that the Δ4, Δ3 R/A, and Δ3 R/D mutants were retained in the ER of SPC18 KO cells.

These results suggested that the Arg residue at the cytoplasm-membrane interface might prevent corin from interacting with ER proteins, including SPC18, with positively charged cytoplasmic residues at or near the membrane (Fig. 5e). In SPC18 KO cells, the cytoplasmic Arg in mWT remained protective, allowing corin expression on the cell surface, whereas the corin mutants without the Arg interacted with ER proteins and, without SPC18 cleavage, were retained in the ER (Fig. 5f).

Analysis of corin proteins in SPC18 KO cells expressing recombinant SPC18 proteins

To verify the importance of the positively charged cytoplasmic residues in SPC18, we generated SPC18 KO cells expressing recombinant SPC18 WT (rSPC18) or a mutant SPC18, in which four positively charged cytoplasmic residues were replaced by Ala residues (SPC18/4A) (Fig. 6a). We analyzed mWT and the mutant corin proteins in these cells. In western blotting, the Cor-p band was detected in mWT and the mutants Δ3 and Δ3 R/K, but not in the mutants Δ4, Δ3 R/A, and Δ3 R/D, in lysates from SPC18 KO cells expressing rSPC18 (Fig. 6b, middle panels), consistent with the findings from parental HEK293 cells (Fig. 5b, c). In contrast, the Cor-p band was not detected in mWT and the corin mutants in lysates from SPC18 KO cells expressing the mutant SPC18/4A (Fig. 6b, middle panels). In the conditioned media from SPC18 KO cells expressing the SPC18/4A mutant, single bands of ~160 kDa with comparable levels were observed in mWT and all the mutants (Fig. 6b, top panels and Supplementary Fig. 7a, b). As a control, rSPC18 and rSPC18/4A protein expression was verified in the transfected SPC18 KO cells (Fig. 6b, bottom panels). These results suggested that mWT corin was cleaved in the ER by SPC18/4A, leading to its secretion and preventing the proper trafficking to the plasma membrane where the activation normally occurred.

Consistently, no overlapping staining of KDEL and corin proteins was observed in SPC18 KO cells expressing either rSPC18 or the mutant SPC18/4A (Fig. 6c and Supplementary Fig. 7c, d). The results indicated that rSPC18 cleaved the corin mutants Δ4, Δ3 R/A, and Δ3 R/D, but not mWT and the mutants Δ3 and Δ3 R/K (Fig. 6d), whereas the mutant SPC18/4A without the positively charged cytoplasmic residues cleaved mWT and all the corin mutants (Fig. 6e).

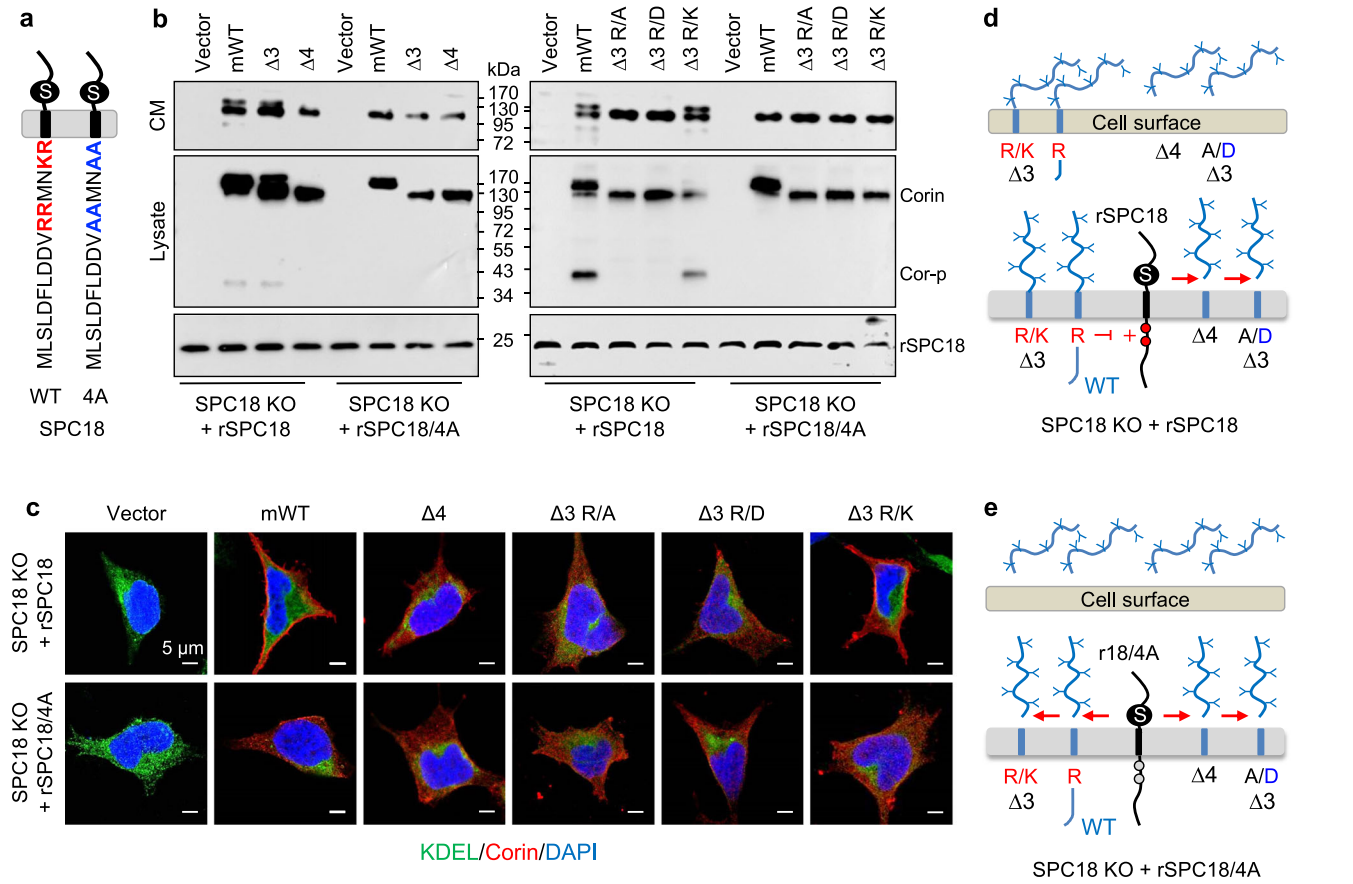

Fig. 6 | Analysis of corin mutants in SPC18 KO cells expressing recombinant SPC18 proteins. a Cytoplasmic sequences in SPC18 WT and the mutant SPC18/4A. **b** Western blotting of corin fragments in the conditioned media (CM) and lysates from SPC18 KO cells expressing recombinant SPC18 WT (rSPC18) or the mutant SPC18/4A (rSPC18/4A). rSPC18 proteins in the transfected cells were verified. Data are representative of at least five experiments. **c** Co-staining of KDEL and corin in SPC18 KO cells expressing rSPC18 or rSPC18/4A. Nuclei were stained with DAPI. Scale bars: 5 μm. Data are representative of at least five experiments. Proposed models. In SPC18 KO cells expressing rSPC18 (**d**), the charge-repulsion mechanism protected corin WT and the mutant Δ3 R/K, but not the mutants Δ4, Δ3 R/A, and Δ3 R/D, from rSPC18 cleavage. Membrane-bound, but not secreted, corin proteins were activated, as indicated by the Cor-p band in western blotting. In SPC18 KO expressing rSPC18/4A (**e**), substitution of the positively charged residues (red dots) with Ala residues (grey dots) at the cytoplasm-membrane interface in SPC18 abolished the protective mechanism, resulting in rSPC18/4A cleavage and secretion of corin WT and all the mutants.

Positively charged cytoplasmic residues in LDLR and matriptase-2

To test if the potential charge-repulsion mechanism observed in corin may apply to other single-pass transmembrane proteins, we analyzed the human LDLR, a type I transmembrane protein in lipid metabolism[46], and human matriptase-2 (also called TMPRSS6), a type II transmembrane protease in iron metabolism[47,48]. Both LDLR (Fig. 7a) and matriptase-2 (Fig. 7b) have positively charged residues at and near the cytoplasm-membrane interface. We mutated those residues to Ala (Fig. 7a, b) and expressed the mutants in HEK293 cells. When the cell lysates were treated with PNGase F and analyzed by western blotting, protein bands from LDLR and matriptase-2 WT and the mutants all migrated faster (Fig. 7c, d), indicating N-glycosylation in these proteins. The results showed that abolishing positively charged residues at and near the cytoplasm-membrane interface in LDLR and matriptase-2 did not alter the membrane topology of LDLR (type I transmembrane protein) or matriptase-2 (type II transmembrane protein).

We next analyzed the LDLR and matriptase-2 WT and the mutants in HEK293 and SPC18 KO cells by flow cytometry. We found that levels of cell surface LDLR WT and the mutant K811A were similar, whereas levels of the LDLR 3A mutant were lower than those of LDLR WT in both HEK293 and SPC18 KO cells (Fig. 7e). Likewise, levels of cell surface matriptase-2 WT and the mutant R52A were similar, whereas levels of the matriptase-2 5A mutant were lower than those of matriptase-2 WT in both HEK293 and SPC18 KO cells (Fig. 7f).

Both LDLR and matriptase-2 undergo ectodomain shedding on the cell surface[49,50]. Consistently, we detected LDLR fragments in the conditioned media from HEK293 and SPC18 KO cells expressing LDLR WT and the mutants (Supplementary Fig. 8a, top panels). There was an extra ~121-kDa band in the conditioned medium from HEK293 cells expressing the 3A mutant (Supplementary Fig. 8a, top left panel), suggesting that the fragment may be from SPC18 cleavage. In the conditioned media from HEK293 and SPC18 KO cells expressing matriptase-2 WT and the mutants R52A and 5A, we found similar matriptase-2 fragments. However, levels of the fragments from the 5A mutant in the conditioned media from SPC18 KO cells appeared lower than those of matriptase-2 WT (Supplementary Fig. 8b, top panels).

In co-immunostaining, there was little overlapping staining between KDEL and LDLR or matriptase-2 proteins in HEK293 cells (Fig. 7g, h, top rows). In SPC18 KO cells, no apparent overlapping staining was observed between KDEL and LDLR WT, the LDLR K811A mutant, matriptase-2 WT or the matriptase-2 R52A mutant (Fig. 7g, h, bottom rows). However, there was strong overlapping staining between KDEL and the LDLR 3A mutant or the matriptase-2 5A mutant in SPC18 KO cells (Fig. 7g, h, bottom rows, and Supplementary Fig. 8c, d). In parallel experiments, there was no apparent co-staining of GM130 and LDLR or matriptase-2 proteins in HEK293 or SPC18 KO cells (Supplementary Fig. 8e, f). These results were consistent with the findings in corin, indicating that the positively charged cytoplasmic residues in LDLR and matriptase-2 were not major determinants in

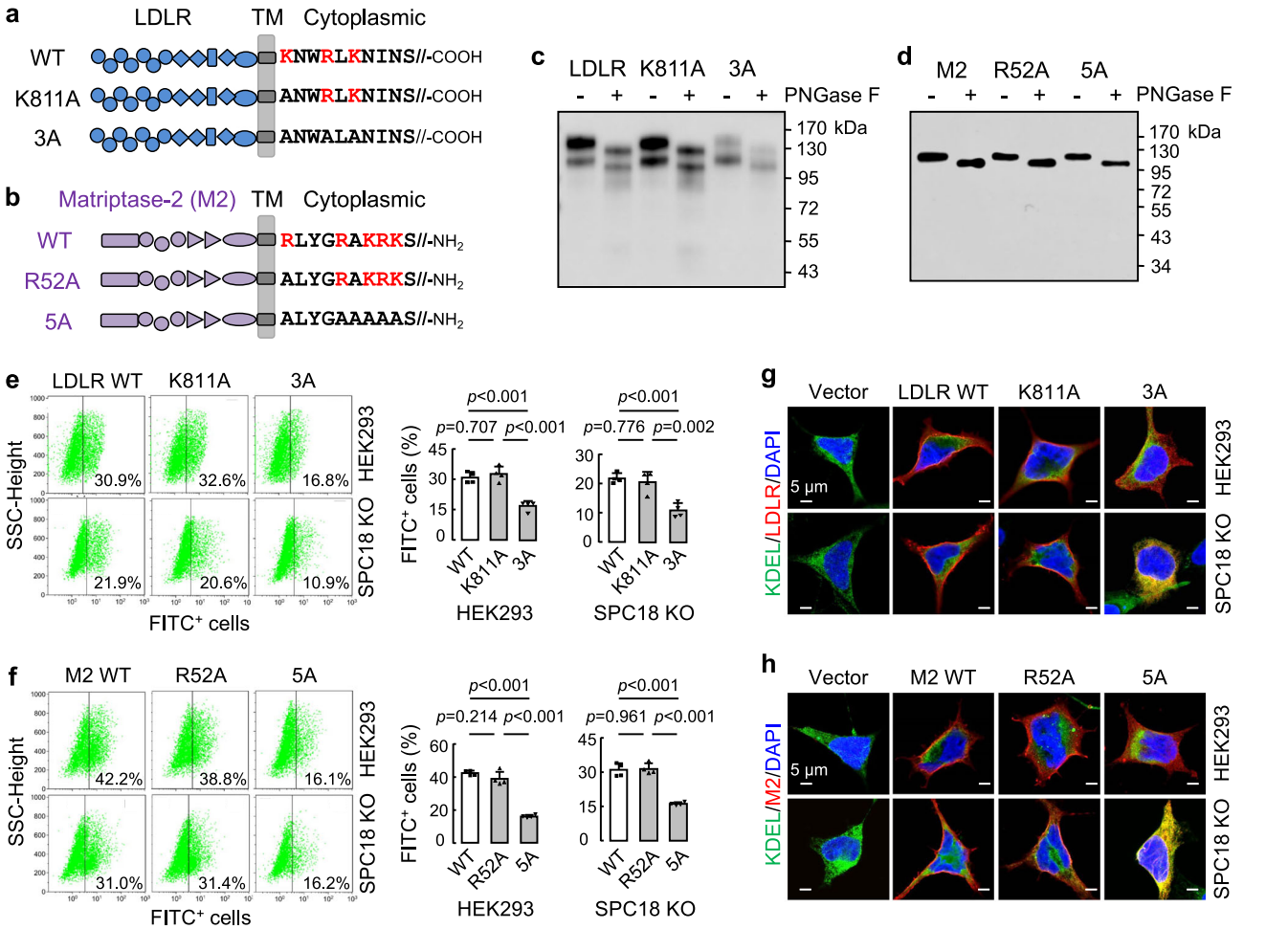

Fig. 7 | ER retention of LDLR and matriptase-2 mutants lacking positively charged cytoplasmic residues. Illustration of human LDLR (**a**) and matriptase-2 (M2) (**b**) domains and partial cytoplasmic sequences with positively charged residues in red. LDLR has a C-terminal cytoplasmic tail, whereas M2 has an N-terminal cytoplasmic tail. LDLR and M2 mutants with mutated cytoplasmic Lys and/or Arg residues are indicated. **c, d** Western blotting of LDLR (**c**) and M2 (**d**) WT and the mutants from HEK293 cell lysates without (−) or with (+) PNGase F treatment. Western blotting was under reducing conditions. Data are representative of three experiments. Flow cytometric analysis of LDLR (**e**) and M2 (**f**) WT and the mutants on the surface of HEK293 and SPC18 KO cells. Quantitative data of LDLR- and M2-positive cells from four experiments are shown in bar graphs. Co-straining of KDEL and LDLR (**g**) or M2 (**h**) proteins in HEK293 and SPC18 KO cells transfected with a vector or plasmids expressing corresponding WT and the mutants. Nuclei were stained with DAPI. Scale bars, 5 μm. Data are representative of at least five experiments.

membrane topology but may serve as a mechanism in preventing abnormal interactions with ER proteins, including SPC18.

Analysis of coirn, LDLR, and matriptase proteins in microsomal fractions

To further verify our findings, we isolated microsomal fractions from HEK293 and SPC18 KO cells expressing corin, LDLR, matriptase-2, and their representative mutants. In western blotting of microsomal proteins, levels of the corin mutant R112D were lower and higher, respectively, than those of mWT from HEK293 and SPC18 KO cells (Fig. 8a, b). As a control, levels of calnexin, an ER chaperone, were comparable in all microsomal preparations (Fig. 8a, second panel). In cell lysates, levels of mWT and the mutant R112D were also comparable (Fig. 8a, third panel). Similar results were found with the LDLR 3A mutant and the matriptase-2 5A mutant, showing that levels of the LDLR 3A mutant (Fig. 8c, d) and the matriptase-2 5A mutant (Fig. 8e, f) were decreased and increased, compared to their WT controls, in the microsomal preparations from HEK293 and SPC18 KO cells, respectively. In controls, levels of microsomal calnexin and LDLR and matriptase-2 proteins were similar between the WTs and the mutants in HEK293 and SPC18 KO cells (Fig. 8c, e, second and third panels). These results supported the idea that corin R112D, LDLR 3A, and matriptase-2 5A mutants were cleaved in the ER in HEK293 cells but retained in the ER in SPC18 KO cells.

Discussion

Studies in proteins from various species have shown that charged residues are important determinants in membrane topology. In *Escherichia coli*, for example, addition or deletion positively charged lysine residues in leader peptidase, a two-pass transmembrane protein, reverses the membrane topology[51,52]. A similar function of charged residues has been reported in seven-transmembrane proteins in the yeast *Saccharomyces cerevisiae*[53,54]. In contrast, the role of charged cytoplasmic residues in membrane orientation of mammalian proteins is less clear. Deletion or substitution of charged residues flanking the transmembrane segment had partial or no effects on the membrane orientation of type I[55] and type II transmembrane proteins[56–60]. These results raise the question regarding the function of the charged cytoplasmic residues in mammalian transmembrane proteins, particularly single-pass transmembrane proteins.

Corin is a type II transmembrane protein conserved in all vertebrates. In this study, we found that one positively charged cytoplasmic residue was sufficient for corin expression on the cell surface. Deletion of the cytoplasmic Arg or substitution of this residue with a neutral or acidic residue

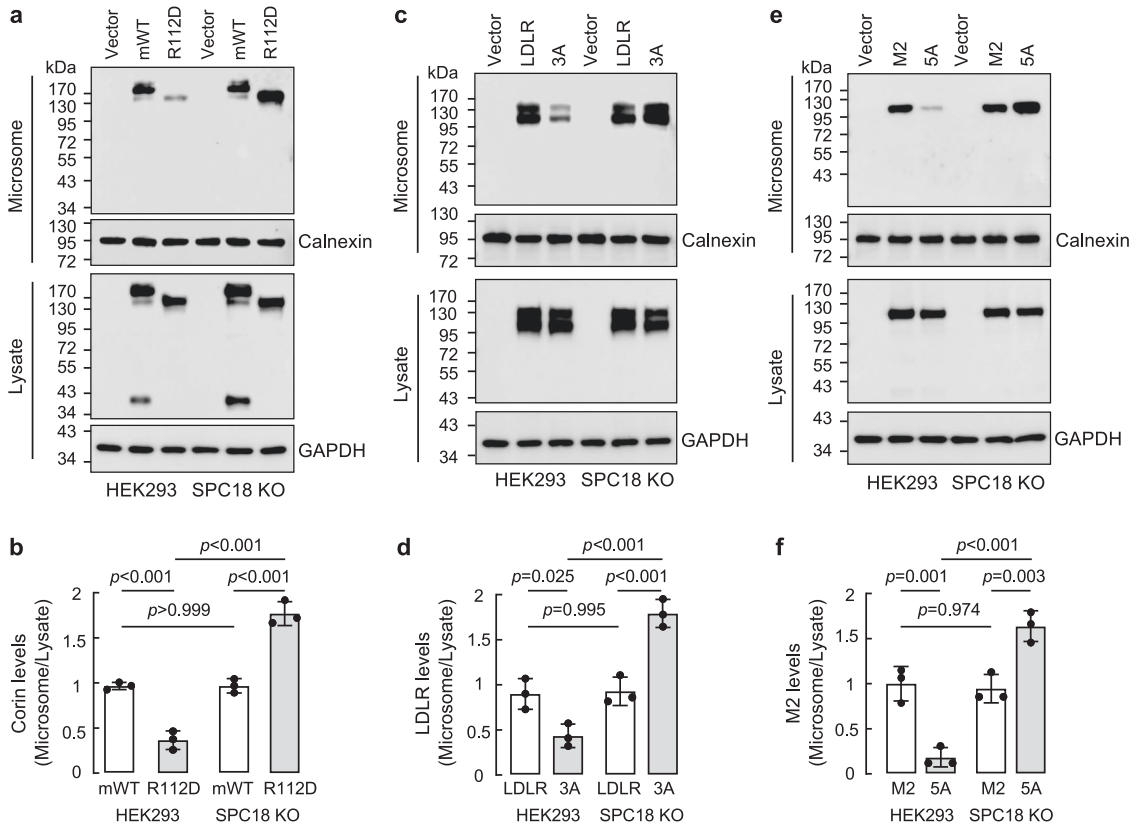

Fig. 8 | Analysis of corin, LDLR, matriptase-2, and their mutants in microsomal fractions. Mouse corin mWT and the mutant R112D (**a**), human LDLR and the mutant 3A (**c**), and human matriptase-2 (M2) and the mutant 5A (**e**) were expressed in HEK293 and SPC18 KO cells. Microsomal fractions were isolated from the cells. Corin, LDLR, and matriptase-2 proteins in the microsomal fractions (top panels) and cell lysates (third panels) were analyzed with western blotting under reducing conditions. Calnexin (second panels) and GAPDH (bottom panels) were loading controls for proteins in the microsomal preparations and cell lysates, respectively. Protein bands on western blots were quantified by densitometry. Levels of microsomal corin (**b**), LDLR (**d**), and matriptase-2 (**f**) proteins were calculated. The data were mean ± S.D. from three experiments, analyzed by one-way ANOVA.

blocked corin cell surface expression. By N-glycosidase digestion, we showed that the corin mutants remained in the type II membrane orientation. Similarly, substitution of positively charged residues with Ala at and near the cytoplasm-membrane interface of human LDLR (type I transmembrane protein) and matriptase-2 (type II transmembrane protein) did not alter their membrane topology, as indicated by N-glycosidase digestion. The presence of soluble fragments from the corin, LDLR and matriptase-2 mutants in the conditioned media from HEK293 cells was consistent with the data from N-glycosidase digestion, showing that the positively charged residues at the cytoplasm-membrane interface were not critical for the membrane topology of these single-pass transmembrane proteins.

We found that the corin mutants, particularly the Δ4 mutant without the cytoplasmic tail and the Δ3 mutants, in which the Arg in the shortened cytoplasmic tail was replaced by a neutral or acidic residue, were secreted from HEK293 cells, resembling sCorin with an engineered signal peptide. These results indicated that the positively charged cytoplasmic residue was not required for corin protein folding, ER exiting, and subsequent intracellular trafficking. Probably, the positively charged residue at the cytoplasm-membrane interface of corin prevented cleavage by the SPC in the ER.

SPC18 and SPC21 are the catalytic subunits of the mammalian SPC paralogs with active residues on the exoplasmic side[42–45]. Based on the single-cell type transcriptomics map of human tissues[61], the SPC paralogs with SPC18 and SPC21 are expressed in most cells. In our study, abolishing SPC18 expression in HEK293 cells blocked the secretion of the corin mutants Δ3 R/A, Δ3 R/D, and Δ4. When recombinant SPC18 was expression in SPC18 KO cells, the secretion of the mutants Δ3 R/A, Δ3 R/D, and Δ4 in the conditioned medium was restored. In contrast, abolishing SPC21 did not block the secretion of the Δ4 mutant from HEK293 cells. These results indicated that the SPC paralogs with SPC18 or SPC21 acted on different sets of proteins and that the cleavage of the corin mutants in HEK293 cells was mediated primarily by SPC18.

In the ER, the SPC is associated with the translocon[62,63]. Previously, secreted type II transmembrane proteins with a shortened cytoplasmic tail or altered transmembrane segment sequences were reported[64–66]. In human invariant chain Iγ of class II histocompatibility antigens, which has an Arg at the cytoplasm-membrane interface, deletion of the entire cytoplasmic tail resulted in the secretion of a truncated Iγ fragment[67]. It was proposed that the transmembrane segment of Iγ may contain a cryptic site and that the deletion of the cytoplasmic tail allowed the transmembrane segment to move upward to the exoplasmic side, thereby exposing the cleavage site to the SPC and resulting in Iγ cleavage and secretion[67]. Thus, the positively charged cytoplasmic residues may restrict vertical movement of the transmembrane segment in the membrane[67]. Based on this model, one would expect that mutant proteins lacking the cytoplasmic tail should remain on the membrane surface of SPC-deficient cells.

In our study, we did not detect the corin mutants Δ3 R/A, Δ3 R/D, and Δ4 on the surface of SPC18 KO cells. Instead, we found that these mutants were retained in the ER of SPC18 KO cells. SPC18 is a type II transmembrane protein with four positively charged residues at and near the cytoplasm-membrane interface[44,45]. These observations suggest a possibility that the positively charged cytoplasmic reside in corin may block lateral interactions with ER proteins, including the SPC, via a charge-repulsion mechanism. Substitution of the Arg at the cytoplasm-membrane interface of

corin with a neutral or acidic, but not basic, residue may compromise this mechanism, allowing SPC18 to cleave corin in the ER. In SPC18 KO cells, the corin mutants were not cleaved but trapped by other ER proteins. In supporting this hypothesis, when the mutant SPC18/4A lacking positively charged residues at the cytoplasm-membrane interface was expressed in SPC18 KO cells, corin WT and the mutants were all cleaved and secreted, but not retained in the ER. In line with findings in corin, similar ER retention was observed when the LDLR and matriptase-2 mutants without the positively charged cytoplasmic residues near the membrane were expressed in SPC18 KO cells. By analyzing microsomal fractions from HEK293 and SPC18 KO cells, we found reduced and increased levels of the corin, LDLR, and matriptase-2 mutants lacking the positively charged residue(s) at the cytoplasm-membrane interface in HEK293 and SPC18 KO cells, respectively. Together, these results suggested that the positively charged cytoplasmic residues in corin, LDLR, and matriptase-2 may protect these proteins from the cleavage by SPC18 and retention in the ER. We would like to point out that the proposed charge-repulsion mechanism may not apply to the positively charged residues in the signal peptide of secreted proteins, which are expected to be buried in the membrane, but not exposed to the cytoplasm. The SPC is known to cleave after the N-terminal signal peptide[45]. LDLR is a type I transmembrane protein with a C-terminal transmembrane segment. In our study, the LDLR 3A mutant lacking the cytoplasmic positive residues also appeared cleaved by SPC18. Further studies will be important to exclude the possibility that the result might be caused by a general indirect impact of a potentially altered ER environment in the transfected cells.

Recently, the SPC has been shown to serve as an important quality control mechanism to remove misfolded membrane proteins in the ER[68]. When cryptic SPC cleavage sites in misfolded membrane proteins are exposed, the SPC degrades defective membrane proteins, thereby maintaining homeostasis in the ER[68]. In principle, the SPC18-mediated cleavage of the corin mutants observed in our study could be part of the membrane protein quality control mechanism. In immunofluorescent staining, however, we did not observe ER retention of the corin mutants in parental HEK293 cells. Additionally, fragments from all the corin mutants were detected in the conditioned media from these cells. These results indicate that the mutant corin proteins were not misfolded in the ER and degraded by the SPC-mediated protein quality control mechanism. Further studies will be important to verify the SPC18-mediated cleavage of the corin mutants and to understand if the observed cleavage in our study may reflect a mechanism to remove off-pathway protein aggregates retained in the ER.

Currently, the identity of the ER proteins that trapped the corin, LDLR, and matriptase-2 mutants in SPC18 KO cells remains unknown. Among mammalian single-pass transmembrane proteins, cytoplasmic sequences in the juxtamembrane region differ greatly[69]. There are no recognizable consensus sequences associated with the positive-inside rule. It is unlikely, therefore, that the corin, LDLR, and matriptase-2 mutants were retained via a mechanism targeting specific protein sequences. More likely, the ER retention was caused by non-specific interactions with ER membrane proteins with positively charged residues at or near the cytoplasm-membrane interface. In principle, soluble cytoplasmic proteins too can interact with the corin, LDLR, and matriptase-2 mutants in SPC18 KO cells. In our study, however, the corin Δ4 mutant, lacking the cytoplasmic tail, was also retained in the ER in SPC18 KO cells, indicating that the protein capture occurred on the exoplasmic side of the membrane.

In summary, positively charged cytoplasmic residues have long been recognized as key determinants in transmembrane protein orientations in many organisms. Our results suggest that positively charged residues at and/or near the cytoplasm-membrane interface in mammalian single-pass transmembrane proteins may not be major determinants in membrane topology. Instead, these residues may provide a mechanism preventing unnecessary protein interactions in the ER membrane. Such a mechanism may not depend on specific protein sequences, which could explain the wide adoption and conservation of the positive-inside rule in diverse transmembrane proteins. It should be pointed that our study focused on mammalian single-pass transmembrane proteins and that the molecular models we proposed are overly simplified, given the fact that mechanisms controlling protein-protein interactions in the ER are complex. Further studies are required to validate our hypothesis and to understand if the findings in this study may apply to other mammalian multi-pass transmembrane proteins. These studies shall help to extend our knowledge regarding the functional significance of the positively charged cytoplasmic residues in transmembrane proteins.

Methods

Expression plasmids

The pcDNA3.1/V5 (Thermo Fisher, K4800-01) based plasmids expressing mouse corin (mWT), human corin (hWT), and human matriptase-2 were published[36,37,50,70]. The full-length human LDLR cDNA was from Origene (RC200006, pCMV6-Entry, with a Flag tag). The full-length human SPC18 cDNA was amplified from HEK293 cells and inserted in the pCMV6-Entry plasmid. Additional corin, matriptase-2, LDLR, and SPC18 mutants were made by site-directed mutagenesis (QuikChange lightning, Agilent Technologies, 210518 or ClonExpress One Step Cloning Kit, Vazyme, C115-01) and verified by DNA sequencing.

Cell culture and transfection

HEK293 cells (ATCC, CRL-1573, STR profiling authenticated) were cultured in Dulbecco's modified Eagle's medium (DMEM) (Corning, 100130CVRC) with 10% fetal bovine serum (FBS) (Gemini, 900-108) at 37 °C with 5% CO_2 and 95% air. To express corin, LDLR, matriptase-2, and SPC18 proteins, the cells at ~70-80% of confluency were transfected with expression plasmids using TurboFect (Thermo Fisher, R0541) or PolyJet (SignaGen Laboratories, SL100688) reagents. The transfected cells were incubated at 37 °C for 5 h and switched to fresh DMEM or Opti-MEM (Thermo Fisher, 31985070). After 30 h, the conditioned medium was collected and the cells were lysed in 1% Triton X-100 (v/v), 50 mM Tris-HCl (pH 8.0), 150 mM NaCl, 10% glycerol (v/v), and a protease inhibitor mixture (1:100 dilution, Roche Applied Science, 04693116001).

Western blotting

Proteins in cell lysates were quantified by NanoDrop2000 and analyzed by SDS-PAGE with (reducing) or without (non-reducing) 2.5% (v/v) β-mercaptoethanol (Sigma-Aldrich, 8.05740) in Laemmli loading buffer after heating at 98 °C for 5 min. Proteins in PAGE gels were transferred to polyvinylidene difluoride membranes (Thermo Fisher). Western blotting was done using a horseradish peroxidase (HRP)-conjugated anti-V5 antibody (1:5000, Thermo Fisher, R96125), HRP-conjugated anti-FLAG antibody (1:10000, Sigma-Aldrich, A8592), an anti-human LDLR antibody (1:200, Abcam, Ab204941, against residues 22-150) and HRP-conjugated secondary antibody (1:10,000, Bioworld, BS22356), or an anti-glyceraldehyde 3-phosphate dehydrogenase (GAPDH) antibody (1:10000, Bioworld, MB001H). Proteins in the conditioned media were concentrated (Millipore, Amicon Ultra 3 K) or immunoprecipitated with anti-V5 antibody-conjugated beads (1:2000, Thermo Fisher, R96025) at 4 °C for 16 h. After washing with phosphate-buffered saline (PBS), proteins were eluted from the beads and analyzed by SDS-PAGE and western blotting. The antibodies used in this study are listed in Supplementary Table 1.

Biotin-labeling of cell surface proteins

HEK293 cells were transfected with corin expressing plasmids and cultured at 37 °C for 24 h. Cell surface proteins were labeled with 1 mM biotin-conjugated sulfo-NHS (0.25 mg/mL) (Thermo Fisher, 21217) at 4 °C for 5 min. The reaction was terminated with glycine (100 mM) in PBS. After 30 min at 4 °C, the cells were lysed. NeutrAvidin Agarose (Thermo Fisher, 89881) were added to the cell lysate and incubated at 4 °C for 2 h. The beads were washed with PBS and heated at 98 °C in a loading buffer for 1 min. Eluted proteins were analyzed by SDS-PAGE and western blotting.

Glycosidase digestion

To examine N-glycans on corin, LDLR, and matriptase-2, glycosidase digestion was conducted with lysates from transfected cells expressing the recombinant proteins. Proteins (120 μg) in denaturing buffer (0.5% SDS and 40 mM dithiothreitol) were boiled for 10 min and treated with 10% (v/v) NP-40 in PBS and PNGase F (30 units, New England Biolabs, P0704S) from *Flavobacterium meningosepticum*, which removes virtually all N-linked oligosaccharides from glycoproteins. After 3 h at 37 °C, the glycosidase-treated proteins were analyzed by SDS-PAGE and western blotting.

Flow cytometry

To examine proteins on the cell surface, HEK293 cells were transfected with expression plasmids and cultured at 37 °C. Similar transfection efficiencies (~ 50%) and comparable protein expression levels of corin, LDLR, matriptase-2, and their mutants were verified by immunostaining and western blotting. After 24 h, the transfected cells were incubated with 0.02% (w/v) EDTA. After 2 min at 37 °C, the detached cells were collected, washed with PBS, and incubated with an anti-V5 antibody (1:1000, Thermo Fisher, R96025) (for corin and matriptase-2 expression) or an anti-human LDLR antibody (1:200, Abcam, Ab204941, against human LDLR residues 22-150). After 1 h at 4 °C, the cells were washed with PBS and incubated with an Alexa Fluor 488-labeled secondary antibody (1:500, Thermo Fisher, A21202) at room temperature in dark for 1 h. After washing with PBS, the cells were examined by flow cytometry (FACSCalibur, BD Biosciences or Gallios, Beckman). Pyridinium iodide (1:1000, Sigma, P8080) was used for life gating. Each experiment was done with duplicated samples and the experiments were repeated at least three times (n ≥ 4). Data were analyzed with FlowJo V7.6.1 or Kaluza software.

Immunofluorescent staining

Subcellular distribution of corin, LDLR, and matriptase-2 was examined with immunofluorescent staining. Transfected cells on coverslips (20 mm in diameter) were fixed with 4% (v/v) paraformaldehyde (cell membrane non-permeable) or pre-cooled acetone (cell membrane permeable) for 5 min at room temperature and incubated with 5% (w/v) BSA in PBS at 37 °C for 1 h. After PBS washing, the cells were co-stained with antibodies against KDEL (1:250, Abcam, ab12223 or 1:500, Abcam, ab176333) or GM130 (1:1000, Abcam, ab52649) and corin (1:300, made in the lab or anti-V5, 1:1000, Thermo Fisher, R96025), LDLR (anti-Flag, 1:500, Sigma-Aldrich, F1804), or matriptase-2 (anti-V5, 1:1000, Thermo Fisher, R96025). Alexa Fluor 488 (Green, 1:500, Thermo Fisher, A21202) or 594 (Red, 1:1000, Thermo Fisher, A11012) conjugated secondary antibodies were used. DAPI (49, 6-diamidino-2-phenylindole dihydrochloride) (Southern Biotech, 0100-20) was used to stain cell nuclei. Immunostaining was examined under a confocal microscope (Olympus, FV3000). Pearson's correlation coefficient analysis was done to examine co-localization of interested proteins and KDEL or GM130.

SPC18/SPC21 KO in HEK293 cells with CRISPR/Cas9

Two pairs of small guide RNAs (sgRNAs) targeting the *SEC11A* gene, encoding SPC18, or the *SEC11C* gene, encoding SPC21, were designed based on the CRISPR/Cas9 website (https://wge.stemcell.sanger.ac.uk//find_crisprs). The following primers were used: gRNA-SPC18-1F (5′-CCG GCG GCA CTA ATG ATC TGG AAG-3′), gRNA-SPC18-1R (5′-AAA CCT TCC AGA TCA TTA GTG CCG-3′), gRNA-SPC18-2F (5′-CCG GTC TCA TCG GCA CTA ATG ATC-3′), gRNA-SPC18-2R (5′-AAA CGA TCA TTA GTG CCG ATG AGA-3′), gRNA-SPC21-1F (5′-CCG GTG ATC GTG TCT TCT GCA CTC-3′), gRNA-SPC21-1R (5′-AAA CGA GTG CAG AAG ACA CGA TCA-3′) and gRNA-SPC21-2F (5′-CCG GTT CCA GTG GCA GTA TGG AGC-3′), gRNA-SPC21-2R (5′-AAA CGC TCC ATA CTG CCA CTG GAA-3′). The primers were cloned into the pGL3-U6-gRNA-Puromycin mut BsaI ACCG plasmid[71]. HEK293 cells were co-transfected with the gRNA plasmids and the pSt1374-N-NLS-3xflag-Cas9-ZF-TM plasmid[71]. The cells were selected with puromycin (0.5 μg/mL) and blasticidin S (16 μg/mL). Disruption of the targeted genes was verified by DNA sequencing. SPC18 and SPC21 protein expression in the KO cells was verified by western blotting with antibodies against SPC18 (1:1000, Sigma-Aldrich, SAB1305956) or SPC21 (1:200, Sigma-Aldrich, HPA026816).

Microsome isolation

Microsome isolation was done using a commercial kit (Abcam, ab206995). Briefly, transfected HEK293 and SPC18 KO cells were detached after trypsin/EDTA treatment and washed with ice-cold PBS. After centrifugation at 700 × g for 5 min, the cell pellets were resuspended in the homogenization buffer (supplied with the kit) and homogenized on ice. The homogenate was centrifuged at 10,000 × g at 4 °C for 15 min. The lipid layer was discarded. The supernatant was collected and centrifuged at 21,000 × g at 4 °C for 20 min. The microsome pellets were washed with the buffer and lysed in 1% Triton X-100 (v/v), 50 mM Tris-HCl (pH 8.0), 150 mM NaCl, 10% glycerol (v/v), and a protease inhibitor mixture (1:100 dilution, Roche Applied Science, 04693116001). Proteins were quantified and analyzed by western blotting. As a control for microsomal proteins, western blots were re-probed with an antibody against calnexin (1:500, ZenBio, 340144) and an HRP-conjugated secondary antibody (1:10,000, Bioworld, BS13278).

Statistics and reproducibility

Prism 8.0 software (Graphpad) was used for the analysis. The data normality was examined using Shapiro-Wilk test. Student's *t* test and ANOVA followed by Tukey's multiple comparison test were used to compare data from two and three or more groups, respectively. P values < 0.05 were statistically significant. All data are presented as means ± S.D.

Reporting summary

Further information on research design is available in the Nature Portfolio Reporting Summary linked to this article.

Data availability

All relevant data are included in the published article and in the supplementary information. Images of the original blots/gels can be found in Supplementary Information and the original data sets used to make bar graphs in Supplementary Data 1. Additional data generated and/or analyzed during this study are available from the corresponding author upon reasonable request. The plasmids used in this study have been deposited in a community repository, as listed in Supplementary information.

Received: 25 May 2024; Accepted: 14 January 2025;
Published online: 20 January 2025

References

1. Almén, M. S., Nordström, K. J., Fredriksson, R. & Schiöth, H. B. Mapping the human membrane proteome: a majority of the human membrane proteins can be classified according to function and evolutionary origin. *BMC Biol.* **7**, 50 (2009).
2. Fagerberg, L., Jonasson, K., von Heijne, G., Uhlén, M. & Berglund, L. Prediction of the human membrane proteome. *Proteomics* **10**, 1141–1149 (2010).
3. Dobson, L., Reményi, I. & Tusnády, G. E. The human transmembrane proteome. *Biol. Direct* **10**, 31 (2015).
4. Hubert, P. et al. Single-spanning transmembrane domains in cell growth and cell-cell interactions: More than meets the eye? *Cell Adh Migr.* **4**, 313–324 (2010).
5. Lomize, A. L., Lomize, M. A., Krolicki, S. R. & Pogozheva, I. D. Membranome: a database for proteome-wide analysis of single-pass membrane proteins. *Nucleic Acids Res.* **45**, D250–D255 (2017).
6. Higy, M., Junne, T. & Spiess, M. Topogenesis of membrane proteins at the endoplasmic reticulum. *Biochemistry* **43**, 12716–12722 (2004).
7. Shao, S. & Hegde, R. S. Membrane protein insertion at the endoplasmic reticulum. *Annu Rev. Cell Dev. Biol.* **27**, 25–56 (2011).
8. von Heijne, G. Membrane-protein topology. *Nat. Rev. Mol. Cell Biol.* **7**, 909–918 (2006).

9. Hartmann, E., Rapoport, T. A. & Lodish, H. F. Predicting the orientation of eukaryotic membrane-spanning proteins. *Proc. Natl Acad. Sci. USA* **86**, 5786–5790 (1989).
10. von Heijne, G. Net N-C charge imbalance may be important for signal sequence function in bacteria. *J. Mol. Biol.* **192**, 287–290 (1986).
11. Von Heijne, G. The distribution of positively charged residues in bacterial inner membrane proteins correlates with the trans-membrane topology. *EMBO J.* **5**, 3021–3027 (1986).
12. Nilsson, J., Persson, B. & von Heijne, G. Comparative analysis of amino acid distributions in integral membrane proteins from 107 genomes. *Proteins* **60**, 606–616 (2005).
13. Wallin, E. & von Heijne, G. Genome-wide analysis of integral membrane proteins from eubacterial, archaean, and eukaryotic organisms. *Protein Sci.* **7**, 1029–1038 (1998).
14. Elazar, A., Weinstein, J. J., Prilusky, J. & Fleishman, S. J. Interplay between hydrophobicity and the positive-inside rule in determining membrane-protein topology. *Proc. Natl Acad. Sci. USA* **113**, 10340–10345 (2016).
15. Peters, C., Tsirigos, K. D., Shu, N. & Elofsson, A. Improved topology prediction using the terminal hydrophobic helices rule. *Bioinformatics* **32**, 1158–1162 (2016).
16. Yan, W., Sheng, N., Seto, M., Morser, J. & Wu, Q. Corin, a mosaic transmembrane serine protease encoded by a novel cDNA from human heart. *J. Biol. Chem.* **274**, 14926–14935 (1999).
17. Ichiki, T. et al. Corin is present in the normal human heart, kidney, and blood, with pro-B-type natriuretic peptide processing in the circulation. *Clin. Chem.* **57**, 40–47 (2011).
18. He, M. et al. The protease corin regulates electrolyte homeostasis in eccrine sweat glands. *PLoS Biol.* **19**, e3001090 (2021).
19. Cui, Y. et al. Role of corin in trophoblast invasion and uterine spiral artery remodelling in pregnancy. *Nature* **484**, 246–250 (2012).
20. Enshell-Seijffers, D., Lindon, C. & Morgan, B. A. The serine protease Corin is a novel modifier of the Agouti pathway. *Development* **135**, 217–225 (2008).
21. Dong, N., Niu, Y., Chen, Y., Sun, S. & Wu, Q. Function and regulation of corin in physiology and disease. *Biochem Soc. Trans.* **48**, 1905–1916 (2020).
22. Zhou, T. et al. Renal Corin Is Essential for Normal Blood Pressure and Sodium Homeostasis. *Int J. Mol. Sci.* **23**, 11251 (2022).
23. Gladysheva, I. P., Sullivan, R. D. & Reed, G. L. Falling corin and ANP activity levels accelerate development of heart failure and cardiac fibrosis. *Front Cardiovasc Med*. **10**, 1120487 (2023).
24. Zhang, X. et al. Corin Deficiency Alters Adipose Tissue Phenotype and Impairs Thermogenesis in Mice. *Biol. (Basel)* **11**, 1101 (2022).
25. Collins, S. A heart-adipose tissue connection in the regulation of energy metabolism. *Nat. Rev. Endocrinol.* **10**, 157–163 (2014).
26. Carper, D. et al. Atrial Natriuretic Peptide Orchestrates a Coordinated Physiological Response to Fuel Non-shivering Thermogenesis. *Cell Rep.* **32**, 108075 (2020).
27. Li, W. et al. Cardiac corin and atrial natriuretic peptide regulate liver glycogen metabolism and glucose homeostasis. *Cardiovasc Diabetol.* **23**, 383 (2024).
28. Zhou, Z. et al. Deficiencies in corin and atrial natriuretic peptide-mediated signaling impair endochondral ossification in bone development. *Commun. Biol.* **7**, 1380 (2024).
29. Zhang, Y. et al. Identification and functional analysis of CORIN variants in hypertensive patients. *Hum. Mutat.* **38**, 1700–1710 (2017).
30. Rame, J. E. et al. Corin I555(P568) allele is associated with enhanced cardiac hypertrophic response to increased systemic afterload. *Hypertension* **49**, 857–864 (2007).
31. Baris Feldman, H. et al. Corin and Left Atrial Cardiomyopathy, Hypertension, Arrhythmia, and Fibrosis. *N. Engl. J. Med*. **389**, 1685–1692 (2023).
32. Zhao, Y. et al. Single-Nucleotide Polymorphisms in the 3' Untranslated Region of CORIN Associated With Cardiovascular Diseases in a Chinese Han Population: A Case-Control Study. *Front Cardiovasc Med*. **8**, 625072 (2021).
33. Zhao, Y. et al. Association of Preablation Plasma Corin Levels With Atrial Fibrillation Recurrence After Catheter Ablation: A Prospective Observational Study. *J. Am. Heart Assoc.* **13**, e031928 (2024).
34. Dong, N. et al. Corin mutations K317E and S472G from preeclamptic patients alter zymogen activation and cell surface targeting. *J. Biol. Chem.* **289**, 17909–17916 (2014).
35. Peng, H. et al. Serum Soluble Corin is Decreased in Stroke. *Stroke* **46**, 1758–1763 (2015).
36. Li, H. et al. A novel cytoplasmic tail motif regulates mouse corin expression on the cell surface. *Biochem Biophys. Res Commun.* **465**, 152–158 (2015).
37. Qi, X., Jiang, J., Zhu, M. & Wu, Q. Human corin isoforms with different cytoplasmic tails that alter cell surface targeting. *J. Biol. Chem.* **286**, 20963–20969 (2011).
38. Zhang, Y. et al. A corin variant identified in hypertensive patients that alters cytoplasmic tail and reduces cell surface expression and activity. *Sci. Rep.* **4**, 7378 (2014).
39. Chen, S. et al. PCSK6-mediated corin activation is essential for normal blood pressure. *Nat. Med.* **21**, 1048–1053 (2015).
40. Jiang, J. et al. Ectodomain shedding and autocleavage of the cardiac membrane protease corin. *J. Biol. Chem.* **286**, 10066–10072 (2011).
41. Niu, Y. et al. Recombinant Soluble Corin Improves Cardiac Function in Mouse Models of Heart Failure. *J. Am. Heart Assoc.* **10**, e019961 (2021).
42. Paetzel, M., Karla, A., Strynadka, N. C. & Dalbey, R. E. Signal peptidases. *Chem. Rev.* **102**, 4549–4580 (2002).
43. Shelness, G. S., Lin, L. & Nicchitta, C. V. Membrane topology and biogenesis of eukaryotic signal peptidase. *J. Biol. Chem.* **268**, 5201–5208 (1993).
44. VanValkenburgh, C., Chen, X., Mullins, C., Fang, H. & Green, N. The catalytic mechanism of endoplasmic reticulum signal peptidase appears to be distinct from most eubacterial signal peptidases. *J. Biol. Chem.* **274**, 11519–11525 (1999).
45. Liaci, A. M. et al. Structure of the human signal peptidase complex reveals the determinants for signal peptide cleavage. *Mol. Cell* **81**, 3934–3948.e3911 (2021).
46. Brown, M. S., Herz, J. & Goldstein, J. L. LDL-receptor structure. Calcium cages, acid baths and recycling receptors. *Nature* **388**, 629–630 (1997).
47. Du, X. et al. The serine protease TMPRSS6 is required to sense iron deficiency. *Science* **320**, 1088–1092 (2008).
48. Ramsay, A. J., Hooper, J. D., Folgueras, A. R., Velasco, G. & López-Otín, C. Matriptase-2 (TMPRSS6): a proteolytic regulator of iron homeostasis. *Haematologica* **94**, 840–849 (2009).
49. Begg, M. J., Sturrock, E. D. & van der Westhuyzen, D. R. Soluble LDL-R are formed by cell surface cleavage in response to phorbol esters. *Eur. J. Biochem* **271**, 524–533 (2004).
50. Jiang, J. et al. N-glycosylation is required for matriptase-2 autoactivation and ectodomain shedding. *J. Biol. Chem.* **289**, 19500–19507 (2014).
51. Nilsson, I. & von Heijne, G. Fine-tuning the topology of a polytopic membrane protein: role of positively and negatively charged amino acids. *Cell* **62**, 1135–1141 (1990).
52. Von Heijne, G. Control of topology and mode of assembly of a polytopic membrane protein by positively charged residues. *Nature* **341**, 456–458 (1989).
53. Goder, V., Junne, T. & Spiess, M. Sec61p contributes to signal sequence orientation according to the positive-inside rule. *Mol. Biol. Cell* **15**, 1470–1478 (2004).
54. Harley, C. A. & Tipper, D. J. The role of charged residues in determining transmembrane protein insertion orientation in yeast. *J. Biol. Chem.* **271**, 24625–24633 (1996).

55. Zuniga, M. C. & Hood, L. E. Clonal variation in cell surface display of an H-2 protein lacking a cytoplasmic tail. *J. Cell Biol.* **102**, 1–10 (1986).
56. Andrews, D. W., Young, J. C., Mirels, L. F. & Czarnota, G. J. The role of the N region in signal sequence and signal-anchor function. *J. Biol. Chem.* **267**, 7761–7769 (1992).
57. Beltzer, J. P. et al. Charged residues are major determinants of the transmembrane orientation of a signal-anchor sequence. *J. Biol. Chem.* **266**, 973–978 (1991).
58. Parks, G. D. & Lamb, R. A. Topology of eukaryotic type II membrane proteins: importance of N-terminal positively charged residues flanking the hydrophobic domain. *Cell* **64**, 777–787 (1991).
59. Stehli, J., Torossi, T. & Ziak, M. Triple arginines in the cytoplasmic tail of endomannosidase are not essential for type II membrane topology and Golgi localization. *Cell Mol. Life Sci.* **65**, 1609–1619 (2008).
60. Wahlberg, J. M. & Spiess, M. Multiple determinants direct the orientation of signal-anchor proteins: the topogenic role of the hydrophobic signal domain. *J. Cell Biol.* **137**, 555–562 (1997).
61. Karlsson, M., et al. A single-cell type transcriptomics map of human tissues. *Sci. Adv*. **7**, eabh2169 (2021).
62. Abell, B. M. et al. Tail-anchored and signal-anchored proteins utilize overlapping pathways during membrane insertion. *J. Biol. Chem.* **278**, 5669–5678 (2003).
63. Kalies, K. U., Rapoport, T. A. & Hartmann, E. The beta subunit of the Sec61 complex facilitates cotranslational protein transport and interacts with the signal peptidase during translocation. *J. Cell Biol.* **141**, 887–894 (1998).
64. Lemire, I., Lazure, C., Crine, P. & Boileau, G. Secretion of a type II integral membrane protein induced by mutation of the transmembrane segment. *Biochem J.* **322**, 335–342 (1997).
65. Roy, P., Chatellard, C., Lemay, G., Crine, P. & Boileau, G. Transformation of the signal peptide/membrane anchor domain of a type II transmembrane protein into a cleavable signal peptide. *J. Biol. Chem.* **268**, 2699–2704 (1993).
66. Schmid, S. R. & Spiess, M. Deletion of the amino-terminal domain of asialoglycoprotein receptor H1 allows cleavage of the internal signal sequence. *J. Biol. Chem.* **263**, 16886–16891 (1988).
67. Lipp, J. & Dobberstein, B. The membrane-spanning segment of invariant chain (I gamma) contains a potentially cleavable signal sequence. *Cell* **46**, 1103–1112 (1986).
68. Zanotti, A. et al. The human signal peptidase complex acts as a quality control enzyme for membrane proteins. *Science* **378**, 996–1000 (2022).
69. Baker, J. A., Wong, W. C., Eisenhaber, B., Warwicker, J. & Eisenhaber, F. Charged residues next to transmembrane regions revisited: “Positive-inside rule” is complemented by the “negative inside depletion/outside enrichment rule. *BMC Biol.* **15**, 66 (2017).
70. Yan, W., Wu, F., Morser, J. & Wu, Q. Corin, a transmembrane cardiac serine protease, acts as a pro-atrial natriuretic peptide-converting enzyme. *Proc. Natl Acad. Sci. USA* **97**, 8525–8529 (2000).
71. Shen, B. et al. Efficient genome modification by CRISPR-Cas9 nickase with minimal off-target effects. *Nat. Methods* **11**, 399–402 (2014).

Acknowledgements

This study was supported in part by grants from the National Natural Science Foundation of China (32171112, 32471158 and 81901499) and Priority Academic Program Development of Jiangsu Higher Education Institutes.

Author contributions

N.D. and Q.W. supervised the study. H.L., S.S., N.D., and Q.W. designed experiments. H.L., S.S., W.G., L.W., Z.Z., Y.Z., C.Z., M.L., S.Z., Y.N., and N.D. performed experiments and collected data. All authors participated in data analysis. H.L., S.S., N.D., and Q.W. wrote the first draft of the manuscript. All authors read and commented on the manuscript and approve the final version for submission.

Competing interests

The authors declare no competing interests.

Additional information

Supplementary information The online version contains supplementary material available at https://doi.org/10.1038/s42003-025-07545-7.

Correspondence and requests for materials should be addressed to Ningzheng Dong or Qingyu Wu.

Peer review information *Communications Biology* thanks the anonymous reviewers for their contribution to the peer review of this work. Primary Handling Editors: Antonio Calabrese and Dario Ummarino.